

# Suppression and Mitigation of Edge Localized Modes in the DIII-D Tokamak with 3D Magnetic Perturbations<sup>\*)</sup>

Todd E. EVANS and the DIII-D Team

*General Atomics, P.O. Box 85608, San Diego, California 92186-5608, USA*

(Received 1 December 2011 / Accepted 7 March 2012)

Uncontrolled Type-I Edge Localize Modes (ELMs) are expected to cause melting of the tungsten divertors in ITER. Methods for controlling ELMs in ITER include pellet pacing and Resonant Magnetic Perturbation (RMP) fields produced by in-vessel, non-axisymmetric, coils. Type-I ELMs have been reproducibly suppressed and mitigated in DIII-D H-mode plasmas with a variety of shapes and pedestal collisionalities using RMP fields of order  $10^{-3} B_T$ . In these experiments the response of Type-I ELMs to applied RMP fields, with a principal toroidal mode number  $n = 3$ , varies dramatically. In some cases there is an evolution in the ELM dynamics involving combinations of small high frequency  $D_\alpha$  spikes mixed with mitigated Type-I ELMs prior to reaching an ELM suppressed state. In other cases, there is continuous change in the frequency and amplitude of the Type-I ELMs. A reduced set of plasma parameters, that significantly affect the dynamics of the ELMs immediately following the application of the RMP field, have been identified. The dynamics of mitigated ELMs are generally consistent with those seen during Type-I through Type-V ELMs although several new types of ELM dynamics have also been observed in plasmas with relatively low toroidal fields as well as during  $q_{95}$  ramps.

© 2012 The Japan Society of Plasma Science and Nuclear Fusion Research

Keywords: edge localized mode, resonant magnetic perturbation, ELM suppression, ELM mitigation, magnetic island, H-mode

DOI: 10.1585/pfr.7.2402046

## 1. Introduction

Edge localized modes (ELMs) are a significant concern for the development of fusion power plants based on the use of toroidal magnetic confinement devices. In ITER a factor of 20–100 reduction in ELM energy impulses on the divertor target plates will be needed to prevent melting of the tungsten surfaces of these components [1, 2]. Since the plasma performance in tokamaks is known to scale with the pedestal temperature when operating in high confinement H-modes and temperature profiles are stiff, the pedestal temperature in ITER will be maintained at a relatively high level compared to existing tokamaks. In addition, the plasma density in ITER must be maintained at the highest possible level throughout the region of the plasma where DT reactions are desired in order to maximize the fusion gain. This implies that a large gradient in the plasma pressure will exist near the edge of the plasma in order to produce a tolerable interface between the plasma and solid surfaces that make up the plasma-facing components such as the first wall and divertor targets.

In DIII-D H-mode plasmas with shapes similar to those planned in ITER, an edge pressure gradient develops that typically covers a region in normalized poloidal magnetic flux ( $\psi_N$ ) of approximately 5%. The large gradient region from the top of the pedestal plasma to the sep-

aratrix provides the energy necessary to destabilize Type-I ELMs [3, 4]. Although ELMs are beneficial for controlling the density and preventing impurities from penetrating through the pedestal into the core plasma in tokamaks such as DIII-D, they release a significant fraction of the energy stored in edge plasma when operating with low electron pedestal collisionalities, i.e.,  $\nu_e^*$  of order 0.3 or less. In plasmas with electron pedestal temperatures ( $T_e$ ) of  $\sim 1$  keV, ion temperatures ( $T_i$ ) of  $\sim 1.5$  keV and line average densities ( $n_e$ ) of  $4 \times 10^{19} \text{ m}^{-3}$ , the total thermal energy stored in the discharge is approximately 1 MJ. During a large Type-I ELM, the pedestal collapses and as much as 20%–30% of the energy stored in the edge of the plasma can be released, resulting in ELM energies of approximately 60 kJ. In DIII-D under some conditions ELMs energies can approach 100 kJ. In ITER the total stored thermal energy is expected to be  $\sim 300$  MJ so an equivalent ELM will release approximately 20–30 MJ. The ITER design limit for tungsten divertor target plates ranges from 0.2 to 1.0 MJ per ELM depending on the assumptions used for the interaction area of the ELMs on the divertor target plates. In ITER, these events are expected to occur with a frequency of 1 Hz for the duration of the ITER discharge. Using these assumptions, we estimate that approximately  $10^5$  ELMs, with an energies of 1 MJ, will degrade the tungsten divertor target plates to the point that they will need to be replaced.

In this paper we describe changes in the dynamics of Type-I ELMs in DIII-D when static  $n = 3$  RMP fields

author's e-mail: [evans@fusion.gat.com](mailto:evans@fusion.gat.com)

<sup>\*)</sup> This article is based on the invited presentation at the 21st International Toki Conference (ITC21).

are applied during discharge with various shapes, normalized plasma pressures ( $\beta_N$ ), collisionalities ( $\nu_e^*$ ) and edge safety factors. In most cases, there is a sequence of transitions in the ELM dynamics before reaching an ELM suppressed state that involves the destabilization various types of ELMs, which do not fit within the standard picture of peeling-ballooning theory [4]. Characterizing the evolution of the ELM dynamics when the RMP field is first applied is important because it gives us insight into the conditions necessary for full ELM suppression. This insight may allow us to optimize RMP ELM suppression in future experiments by improving the design of RMP coils or provide a path leading to the development of alternative ELM suppression techniques. It is also important to understand the physics of the transition from Type-I ELMs to the ELM suppressed state during the initial application of the RMP field in order to minimize the size and number of ELMs during this period since these contribute to the inventory of ELMs that will be allowed in ITER before reaching the final erosion limit of the divertor target plates.

## 2. RMP ELM Mitigation and Suppression in Low Collisionality DIII-D Plasmas

Resonant Magnetic Perturbation (RMP) fields produce a range of differing ELM responses in DIII-D depending on  $\nu_e^*$ , the configuration of the RMP coil, the plasma shape,  $\beta_N$  and the value of the safety factor at  $\psi_N = 0.95$  ( $q_{95}$ ). It is important to distinguish between these various types of ELM response since in ITER a reduction in the ELM size may be sufficient for some operating scenarios while a complete elimination of the ELMs may be necessary in others. In low collisionality ( $\nu_e^* \sim 0.18$ ), lower single-null, plasmas with lower triangularities of  $\delta_1 = 0.37$ , as shown in Fig. 1, ELMs are mitigated when the RMP field is applied with  $q_{95} > 3.7$ . In these discharges, with  $\beta_N = 2.2$  and an injected neutral beam power  $P_{inj} = 7.9$  MW, ELMs transition from large well defined Type-I dynamics to a mixture of smaller Type-I ELMs with a slightly higher frequency than those during the pre-RMP phase and then to much smaller ELMs with a significantly higher frequency. This transition in the ELM dynamics is shown in Fig. 2. A series of distinct dynamical states are seen in the divertor  $D_\alpha$  signals as the RMP field is ramped to its steady-state level and  $q_{95}$  crosses 3.7. First, we note that when the RMP field is initially applied at  $t = 1.50$  s there is an immediate reduction in the average size of the Type-I ELMs along with an increase in their frequency. This behavior persists until  $t = 1.58$  s.

During the first 50 ms of this period the RMP field is being ramped up linearly to its steady-state value with an RMP coil current of 3 kA and the pedestal density drops from  $3.2 \times 10^{19} \text{ m}^{-3}$  to  $2.8 \times 10^{19} \text{ m}^{-3}$ . Between  $t = 1.55$  s and 2.05 s all the plasma parameters are held constant except  $q_{95}$  which slowly drops from 4.0 to 3.7. At  $t = 1.58$  s

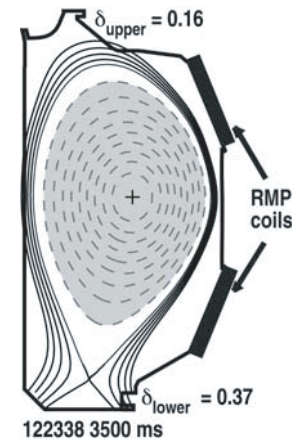


Fig. 1 Low triangularity, lower single null, plasma shape used for most low electron pedestal collisionality RMP experiments prior to 2006.

the ELMs begin to transition to a new dynamical state. During this transition small spikes appear early in the post-crash recovery phase of the Type-I ELMs. These spikes apparently act to inhibit the formation of some Type-I ELMs, which reduces their overall frequency. These small spiky ELMs are similar to Type-II ELMs [5] which typically occur at higher  $\nu_e^*$  and to Type-III ELMs [6] which are observed at lower power levels near the L-H power threshold. By  $t = 1.65$  s the small spiky ELMs dominate the  $D_\alpha$  dynamics between the larger Type-I ELMs and then gradually disappear in the early post-crash phase. By 1.85 s the small  $D_\alpha$  spikes are almost entirely gone between the Type-I ELMs and at  $\sim 1.89$  s, as  $q_{95}$  crosses 3.75 the Type-I ELMs are completely suppressed. The suppression seen between 1.89 and 2.10 s is marginal since several random Type-I ELMs are observed in the  $D_\alpha$  signal. Beyond  $t = 2.10$  s all of the ELMs large and small are completely eliminated. We refer to the phase between  $t = 1.50$  and 1.89 s as ELM mitigation, the period between 1.89 and 2.10 s as marginal suppression and the period after  $t = 2.10$  s as full suppression. We refer to the fully suppressed state as an RMP H-mode or an ELM suppressed plasma.

In matched discharges with the same parameters as 122338 and  $\beta_N = 1.4$  ( $P_{inj} = 4.2$  MW), the evolution of the ELM dynamics is significantly different than in the  $\beta_N = 2.2$  case and the final state is marginally suppressed rather than fully suppressed. This change can be seen in Fig. 3 during DIII-D discharge 122343. In this case the mitigated ELMing phase lasts longer and the Type-I ELMs have a different character later in the mitigation phase. The average size of the mitigated ELMs in the  $\beta_N = 1.4$  discharge is  $\sim 25\%$  larger than in the  $\beta_N = 2.2$  discharge prior to  $t = 2.0$  s and increases somewhat between 2.2 and 2.4 s. In addition, the Type-I ELMs seen after  $t = 2.0$  s have significant excursions below the baseline  $D_\alpha$  level which are not as obvious in the  $\beta_N = 2.2$  discharge. The small spiky, Type-II-like, ELMs are much less apparent in the lower  $\beta_N$

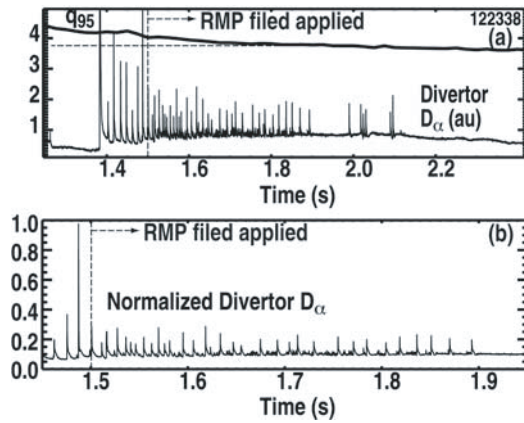


Fig. 2 (a) Time evolution of the  $q_{95}$  and lower divertor recycling ( $D_{\alpha}$ ) signals in discharge 122338, (b) an expanded view of the ELM dynamics with the ELMs normalized to the Type-I ELM seen just before the RMP field is applied showing a sequence of transitions in ELM dynamics as  $q_{95}$  is reduced with RMP field applied.

discharge and do not appear to have a significant impact on the Type-I dynamics. In discharge 122343, the mitigated ELM phase persists until approximately 2.4 s and then appears to transition into a marginally ELM suppressed state although the transition is not particularly well defined due to the occurrence of a Type-I ELM at  $t = 2.5$  s followed by a 0.82 s quiescent period without any Type-I ELMs. During the marginally suppressed state the ELMs are about 35% larger than the earlier mitigated ELM and appear somewhat randomly with no indication of a distinct trigger in any of the background pedestal parameters. In particular, there is no apparent correlation between these ELMs and core MHD activity, which is sometimes seen during the return of Type-I ELMs in other operating regimes as discussed in Ref. [7].

A matched discharge with  $\beta_N = 1.7$  ( $P_{inj} = 5.0$  MW) has an evolution in the ELM dynamics that shares some of the properties seen in both the  $\beta_N = 2.2$  and the  $\beta_N = 1.4$  discharges. Figure 4 shows the lower divertor recycling ( $D_{\alpha}$ ) evolution in discharge 122342 where the ELM mitigated phase persists until 2.42 s followed by a clear transition into an RMP H-mode with full ELM suppression. When the RMP field is applied there is a 0.5 s long period of relatively high frequency Type-I mitigated ELMs followed by a gradual reduction in frequency over the next 0.4 s and a transition into the ELM suppressed phase at  $t = 2.4$  s.

Beginning with the first plasma in the 2006 DIII-D operations period, the lower divertor shelf was extended inward toward the center-post to allow efficient neutral particle pumping in a higher triangularity lower single-null plasma shapes similar to that planned for the 15 MA ITER H-mode scenario. Figure 5 shows the shape of a generic ITER Similar Shaped (ISS) plasma used for most low  $\nu_e^*$  RMP ELM suppression experiments since this change in

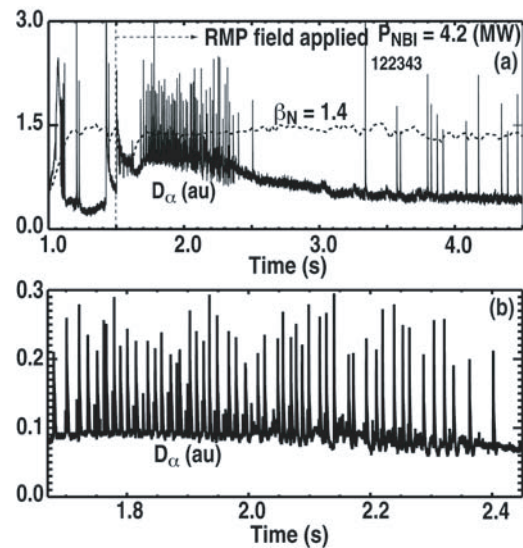


Fig. 3 (a) Time evolution of  $\beta_N$  and lower divertor recycling ( $D_{\alpha}$ ) signals in discharge 122343 following the application of RMP fields as  $q_{95}$  is reduced with  $\beta_N = 1.4$  showing marginal ELM suppression after 2.5 s, (b) an expanded view of the ELM dynamics with the ELMs normalized to the largest Type-I ELM seen before the RMP field is applied in (a) showing a sequence of transitions in ELM dynamics while the RMP field applied.

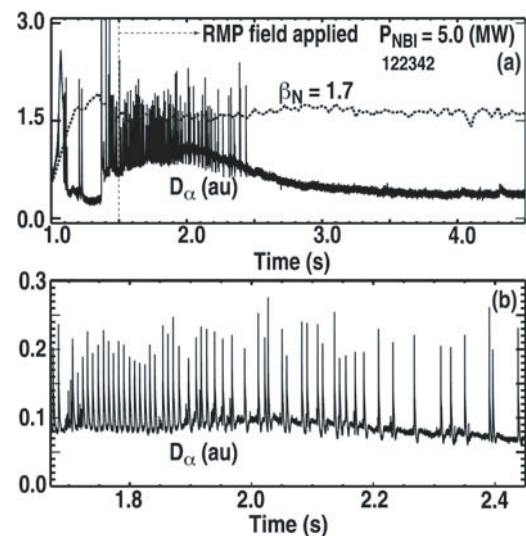


Fig. 4 (a) Time evolution of  $\beta_N$  and lower divertor recycling ( $D_{\alpha}$ ) signals in discharge 122342 following the application of RMP fields as  $q_{95}$  is reduced with  $\beta_N = 1.7$ , (b) an expanded view of the ELM dynamics with the ELMs normalized to the largest Type-I ELM seen before the RMP field is applied in (a) showing a sequence of transitions in ELM dynamics while the RMP field applied.

the lower divertor configuration. As discussed in Ref. [7] significant differences are observed between the pre-2006 lower single null and post-2006 plasma response to the applied RMP fields from the RMP coil. In general, the mitigated ELM behavior also changed with the new divertor

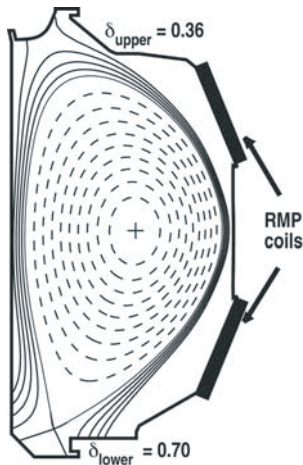


Fig. 5 Generic ISS plasma used in DIII-D beginning in 2006 for most RMP experiments.

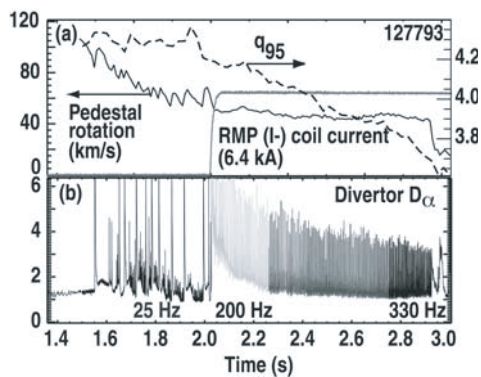


Fig. 6 (a)  $q_{95}$ , pedestal rotation and RMP (I-) coil current variations leading to (b) ELM mitigation in discharge 127793 with an increase in the Type-I ELM frequency from  $f_{\text{ELM}} = 200$  Hz (light gray) to  $f_{\text{ELM}} = 330$  Hz (black). The dark gray region between 200 Hz and 330 Hz is a period in which the frequency of the Type-I ELMs is increasing continuously and the amplitude is decreasing approximately as  $f_{\text{ELM}}^{-1}$ .

geometry along with the recycling behavior as discussed in Ref. [8]. In particular, it was found that full ELM suppression in ISS plasmas requires about 25% more RMP coil current in most parameter regimes studied. It was also found that the  $q_{95}$  window over which RMP H-modes were observed is somewhat smaller and centered near  $q_{95} = 3.45$ . Several new ELM mitigation regimes have also been observed in ISS plasmas. For example, a mode of operations has been identified in which the frequency of mitigated Type-I ELMs and their amplitude evolves continuously as  $q_{95}$  is ramped down i.e., with the plasma current ramped up and  $B_T$  held constant. This behavior is shown in Fig. 6.

Here, the RMP field is applied with  $q_{95}$  at approximately 4.2 during the ramp. As seen in Fig. 6 (a) the baseline recycling signal increases promptly and then decays

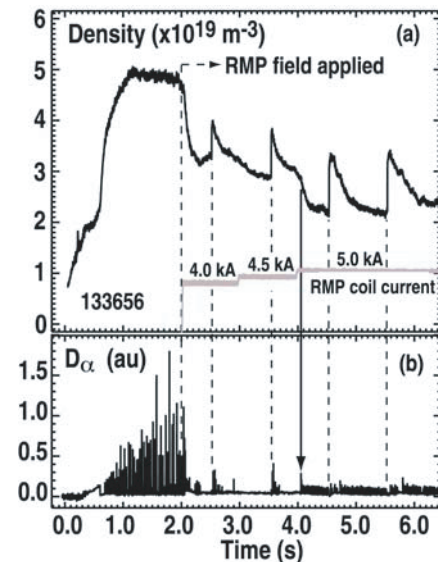


Fig. 7 Time evolution of (a) line averaged density and RMP (I-) coil current (gray) normalize to 5 kA, (b) lower divertor recycling signal in an RMP ELM suppressed discharge with  $B_T = -1.58$  T. Dashed lines at  $t = 2.5, 3.5, 4.5$  and  $5.5$  s indicate times when  $D_2$  fueling pellets are injected.

rather slowly back to its original level i.e., within about 0.3 s. At the same time, the 25 Hz Type-I ELMs, seen prior to the applied RMP field, immediately transition to a frequency of  $\sim 200$  Hz. As  $q_{95}$  continues to drop the frequency of the Type-I ELMs increases and there is a modest decrease in their amplitude. By 2.8 s the frequency has increased to 330 Hz. Shortly after this,  $q_{95}$  reaches the upper end of the usual ELM suppression window observed in this configuration and a locked mode is triggered terminating the discharge.

As shown in Fig. 6 (a) the toroidal rotation at the top of the pedestal remains constant at about 40 km/s during the mitigation phase and then drops sharply when the locked mode forms. This behavior is sometimes observed when counter neutral beam torque is applied to ELM suppressed plasmas with pedestal rotations near 40 km/s. As discussed in Ref. [7], when the pedestal rotation drops into this range, during the application of counter-NBI torque, large core neoclassical tearing modes (NTMs) are triggered that rapidly spin down and lock causing a plasma current disruption although this is not typically observed during our usual co-NBI heated RMP suppressed cases. It should be noted that during the mitigated ELM phase in this discharge the line average density is also dropping substantially which may be influencing the ELM dynamics and is most likely contributing to the onset of the locked mode.

Another distinct type of ELM dynamics seen in ISS plasmas is shown in Fig. 7. In this discharge the toroidal field was  $-1.58$  T with  $q_{95} = 3.56$  and  $P_{\text{inj}} = 7.55$  MW ( $\beta_N = 1.6$  during the RMP phase). Most ISS ELM suppression experiments, such as those discussed above, are carried out

with  $B_T$  between  $-1.9$  and  $-2.0$  T but in this case  $B_T$  was reduced to study the effects of the RMP field on the plasma response at across a range of toroidal fields. In discharge 133656, the RMP field is applied at  $t = 2.0$  s with an initial current of 4 kA. At 3.0 s the RMP coil current is stepped up to 4.5 kA and at 4.0 s to 5.0 kA. The initial ELM response is fairly typical of that seen in higher  $B_T$  experiments with similar plasma parameters and coil currents although there is an initial sharp drop in the line average density ( $n_e$ ). This reduction in  $n_e$  is significantly larger than  $n_e$  reductions that are typically seen in ISS plasmas at higher  $B_T$ .

Referring to Fig. 7, we see that Type-I ELMs are immediately mitigated by the RMP field and after a few ELM cycles transition to a marginally suppressed state. This is followed by a short burst of small ELMs with properties that are very similar to Type-I ELMs in which the  $D_\alpha$  signals have a very fast,  $< 50 \mu\text{s}$ , rise time followed by a slow decay back to the baseline level as the pedestal pressure recovers. At 2.5 s, a deuterium fueling pellet is injected into the discharge. There is an associated  $D_\alpha$  burst, which is sometime seen during pellet fueling in ISS plasmas [7]. This is followed by a short period of small, mitigated, ELMs. At this point in the discharge  $n_e$  is slightly above  $3 \times 10^{19} \text{ m}^{-3}$  and still well above the L-mode density of  $2 \times 10^{19} \text{ m}^{-3}$  just before the H-mode transition at 0.6 s. When the RMP coil current is stepped up to 4.5 kA at 3.0 s there is a relatively slow decay in  $n_e$  to a new equilibrium value of  $2.7 \times 10^{19} \text{ m}^{-3}$ . During this time, from 3.0 s to 3.5 s, the plasma remains in a marginally suppressed state. At 3.5 s a second fueling pellet is injected. This pellet produces a response in the  $D_\alpha$  signal similar to that of the first pellet. Then at 4.0 s a step to 5.0 kA in the ELM coil current triggers a rapid reduction in  $n_e$  to  $2.3 \times 10^{19} \text{ m}^{-3}$ . At this point the discharge is relatively close to the L-mode density seen earlier in the discharge and there is very little pedestal pressure left to drive peeling-ballooning modes although a weak transport barrier still exists and the plasma remains in an H-mode.

The  $D_\alpha$  signal in the phase after 4.0 s is quite extraordinary. First, we note that there is a sharp  $D_\alpha$  spike associated with the RMP coil current step at that time and an abrupt drop in  $n_e$  immediately following the current step followed by a somewhat continuous, moderately high frequency, sequence of small ELM-like bursts. Since the pedestal pressure gradient is very small and well below the ballooning stability boundary believed to be responsible for Type-I ELMs, it is reasonable to hypothesize that these events are not mitigated Type-I ELMs but some other type of small low-density ELM. It is possible that they are related to low  $n_e$  Type-IV ELMs [9] or they may be similar to Type-V ELMs observed in NSTX [10]. It is curious that fueling pellets injected into this plasma cause an interruption in these small  $D_\alpha$  events similar to the typical ELM-free phase associated with L-H transitions. In addition, the decay rate in  $n_e$  following each fueling pellet in this phase of the discharge is significantly slower than that

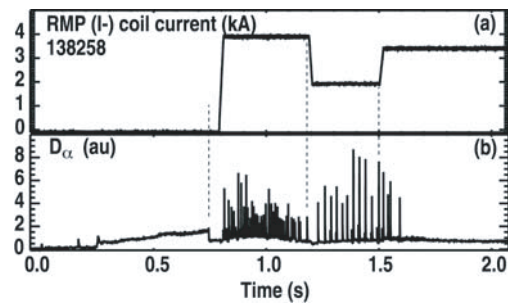


Fig. 8 (a) RMP coil current waveform and (b) response of the lower divertor  $D_\alpha$  signal behavior to the RMP field.

of the previous two fueling pellets.

The RMP coil current also has an effect on the dynamics of ELMs immediately following the L-H transition as shown in Fig. 8. Here, the coil is applied during the ELM-free phase following the transition to an H-mode. During the initial RMP phase, with a 4.0 kA current, ELMs are mitigated i.e., they transition to a lower amplitude with a higher frequency. At 1.2 s the coil current is reduced to 2.0 kA allowing large Type-I ELMs to form. Then at 1.5 s the coil current is increased to 3.4 kA and after several Type-I ELM cycles suppression is obtained.

In ITER it may be necessary to apply RMP fields either before the L-H transition or during the ELM-free phase in order to suppress the first ELM. This has been done in DIII-D ISS plasmas as shown in Fig. 9. Here, we see that the density, Fig. 9 (a), is reduced during the ELM-free phase by the RMP field in discharge 140288 (black trace) compared to discharge 140133 (gray trace) with the application of a larger RMP (I-) coil current as shown in Fig. 9 (b). The discharge with the higher RMP field has a delayed H-mode transition as indicated by the H-mode quality parameter ( $H_{98y2}$ ) crossing 1.0 in Fig. 9 (c). Comparing the lower divertor  $D_\alpha$  signals i.e., Fig. 9 (d) and 9 (e) in these two discharges, we see that Type-I ELMs are suppressed immediately following the L-H transition in the discharge with the higher RMP coil current as shown in Fig. 9 (e). The small oscillations seen in Fig. 9 (e) immediately following the H-mode transition are due to a sequence of L-H and H-L transition in discharge 140228 due to the close proximity of  $P_{inj}$  to the H-mode power threshold. The evolution of  $P_{inj}$  for these two discharges is shown in Fig. 9 (f) where we see that the power demand due to the  $\beta_N$  feedback algorithm is lower in the discharge with the higher RMP field.

Here, we note that a key distinction between ELM-free discharges and RMP ELM suppressed discharges is the ability of the RMP fields to control the density, impurity influx and radiated power. Density and impurity control is essential for steady-state operations in ITER. ELM-free discharges characteristically have an uncontrolled density rise accompanied by an accumulation of impurities in the core plasma. This can lead to a radiative collapse and a disruptive termination of the plasma current,

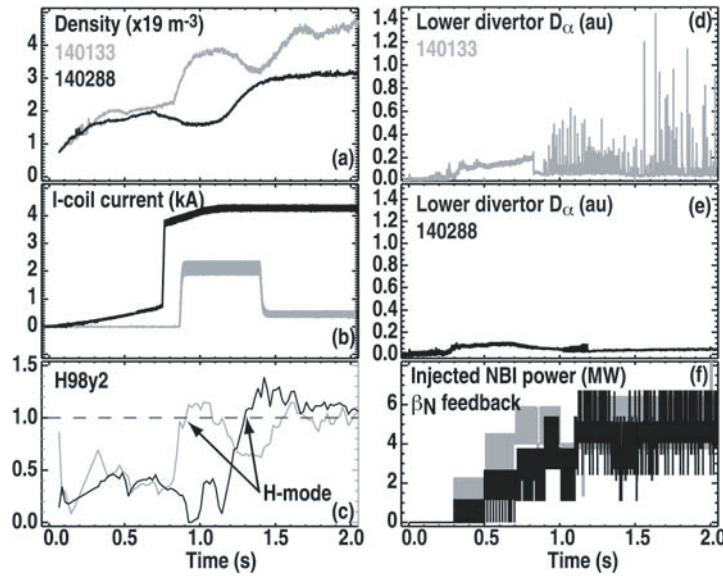


Fig. 9 (a) Line average density, (b) RMP (I-) coil current, (c) H98y2 H-mode quality factor, (d)  $D_\alpha$  signal in discharge 140133, (e)  $D_\alpha$  signal in discharge 140288 and (f)  $P_{inj}$ .

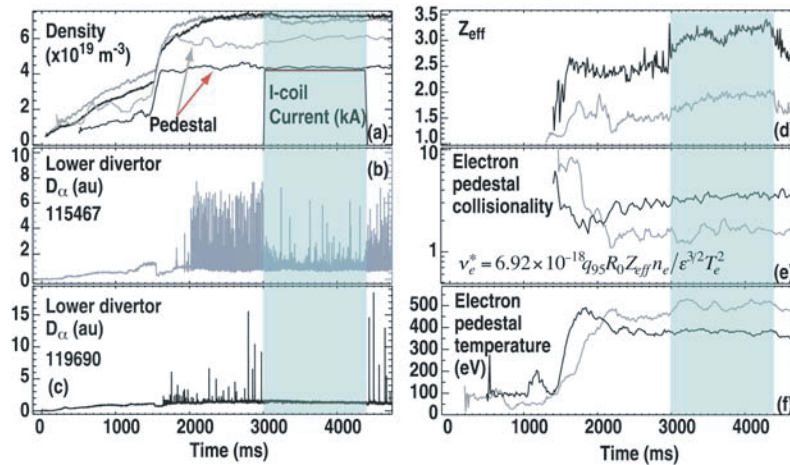


Fig. 10 (a) Line average density, upper traces, RMP (I-) coil current bracketing the shaded region and pedestal density for discharges 115467 (gray) and 119690 (black), (b) lower divertor  $D_\alpha$  signal for 115467, (c) lower divertor  $D_\alpha$  signal for 119690, (d) pedestal  $Z_{eff}$ , (e)  $\nu_e^*$ , and (f) pedestal electron temperature for these two discharges.

which in ITER is expected to generate large levels of MeV runaway electron current. Large levels of MeV runaway electrons will damage in-vessel components in ITER unless they can be mitigated or suppressed.

### 3. RMP ELM Suppression in High Collisionality DIII-D Plasmas

The first demonstration of Type-I ELM suppression using RMP fields was done in high electron pedestal collisionality DIII-D discharges with  $\nu_e^* > 0.9$  [11, 12]. In these experiments the applied RMP fields were approximately an order of magnitude smaller than those in the low electron pedestal collisionality discharges discussed above. Recently, similar results were obtained in ASDEX-

Upgrade [13]. Figure 10 shows a comparison between two high  $\nu_e^*$  discharges with marginal and full ELM suppression. As seen in Fig. 10(a) there is no reduction in the line average or the pedestal  $n_e$  during the application of the RMP field. Discharge 115467 is an example of a marginally suppressed case. As seen in Fig. 10(b), the  $D_\alpha$  signal has several Type-I ELMs that are randomly separated by small, low frequency, modulations of the baseline. As discussed below, these modulations have significantly different properties than those seen during ELMs and appear to result from a very different type of plasma dynamic.

Figure 10(c) shows the  $D_\alpha$  response observed during Type-I ELM suppression in these discharges. Unlike the low  $\nu_e^*$  discharges discussed above, there is no transition through an ELM mitigated state when the RMP field

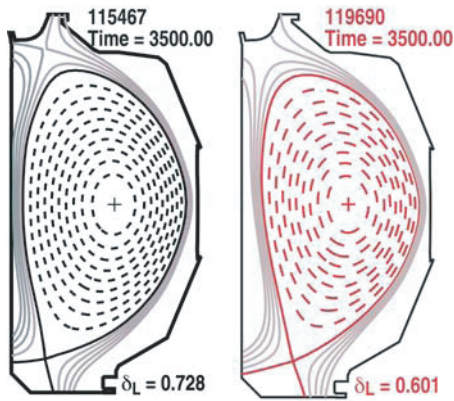


Fig. 11 Plasma shape for discharge 115467 (left) and 119690 (right) used during high collisionality RMP ELM suppression experiments in DIII-D.

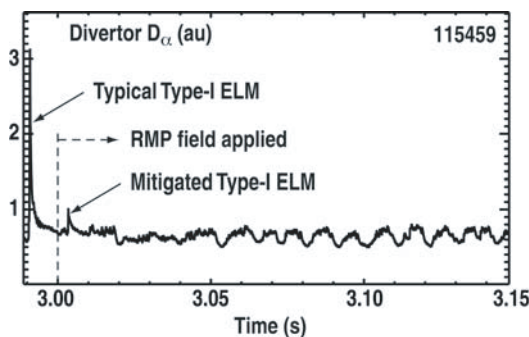


Fig. 12 Oscillations in the lower divertor  $D_\alpha$  signal following the application of the RMP field at 3.0 s.

is applied. Instead the plasma goes immediately into an ELM suppressed state. Differences in the pedestal  $Z_{\text{eff}}$ ,  $\nu_e^*$  and the electron pedestal temperature for these two cases are shown in Figs. 10(d,e,f), respectively. Other than the differences shown in Fig. 10 for these two cases, there is a significant difference in the plasma shapes. Figure 11 (left) shows the plasma shape in discharge 115467 and Fig. 11 (right) shows the plasma shape in discharge 119690. Note the differences in the lower triangularity and the lower inner gap. Discharge 119690 is modeled after the 15 MA ITER H-mode scenario 2 configuration.

Figure 12 shows details of changes in the  $D_\alpha$  signal in a discharge with plasma and RMP field parameters matched to those of discharge 115467 shown in Fig. 10 (b). In this discharge we see a single Type-I mitigated ELM following the application of the RMP field. Note that this mitigated ELM is about a factor of 3 smaller than the Type-I ELM seen just before the RMP field is applied. The discharge quickly transitions into a dynamical state with small low frequency coherent  $D_\alpha$  oscillations. It is important to note that these oscillations have moderately slow rise times compared to ELMs. This is significant because it is the fast transient nature of the ELMs, that drive large energy impulses, which causes melting and erosion of solid surfaces

in ITER. Thus, the behavior seen in these high  $\nu_e^*$  RMP discharges is referred to as marginal ELM suppressed rather than ELM mitigation.

## 4. Discussion and Conclusions

A wide range of ELM dynamics are observed during RMP experiments in DIII-D plasmas with differing shapes, edge safety factors ( $q_{95}$ ), normalize plasma pressures ( $\beta_N$ ) and electron pedestal collisionalities ( $\nu_e^*$ ). Many of these are consistent with behaviors attributed either to Type-I, II, III, IV or V ELMs that occur spontaneously in H-mode discharges. In addition, several new types of  $D_\alpha$  dynamics are observed during the application of RMP fields that do not appear to correlate with these standard types of ELMs. In some cases, for example in high  $\nu_e^*$  discharges, the applied RMP field is approximately equal to the known field-errors from the poloidal field coils in combination with stray fields from the toroidal field bus connections in DIII-D. This implies the possibility that the dynamics of some types of naturally occurring ELMs may be influenced or even dominated by intrinsic field-errors in tokamaks. RMP fields, controlled by currents in non-axisymmetric coils e.g., the internal RMP coil in DIII-D, are a valuable tool for altering the dynamics of ELMs in order to carry out detailed physics studies of their properties.

It is important to understand the evolution of the ELM dynamics in various plasma shapes, collisionality regimes and as a function of  $q_{95}$  or  $\beta_N$  when the RMP field is first applied since in most cases the final ELM suppressed state is preceded by a finite period with ELMs of one type or another. In ITER, it will be necessary to minimize the size and number of ELMs during the period prior to the suppressed state since these ELMs will reduce the lifetime of the divertor target plates. In addition, a key physics question to be addresses is whether it is necessary to undergo some form of dynamical transition in the behavior of the ELMs before reaching full suppression. As shown in Fig. 10(a) above, there are cases where ELM suppression is obtained without undergoing any change in dynamics. We also see in Fig. 9 (e) that when the RMP field is applied prior to the L-H transition, there is a short period with multiple transitions into and out of an H-mode, so-called dithering, without triggering any ELMs whatsoever.

Finally, it is noted that some measurements indicate a locking of the mitigated ELMs to the applied  $n = 3$  RMP field. This leads to the question of whether these mitigated ELMs are fixed in space and periodically release a burst of heat and particles as they reach some limit that is well below the usual peeling-ballooning instability boundary or whether they rotate with the plasma and only release their energy when their helical phase matches that of the external RMP field. Developing a better understanding of this process during the various types of ELM evolution discussed above may lead to a more comprehensive model of how the final ELM suppressed state is achieved when the RMP field is applied. In particular, a model recently pro-

posed suggests that thermoelectric currents driven in homoclinic tangles produced by external RMP fields could explain the evolution of the ELM dynamics seen prior to reaching the fully suppressed state [14]. Work is continuing to compare the predictions prescribed by this model with experimental measurements.

## Acknowledgments

This work was supported by the US Department of Energy under DE-FC02-04ER54698.

- [1] A. Loarte *et al.*, Plasma Phys. Control. Fusion **45**, 1549 (2003).
- [2] R. Pitts, personal communication (2011).
- [3] H. Zohm, Plasma Phys. Control. Fusion **38**, 105 (1996).
- [4] P.B. Snyder *et al.*, Phys. Plasmas **12**, 056115:1 (2005).
- [5] J. Stober *et al.*, Nucl. Fusion **41**, 1123 (2001).
- [6] R. Sartori *et al.*, Plasma Phys. Control. Fusion **46**, 723 (2004).
- [7] T.E. Evans *et al.*, Nucl. Fusion **48**, 024002 (2008).
- [8] E.A. Unterberg *et al.*, J. Nucl. Mater. **390-391**, 486 (2009).
- [9] A. Kirk *et al.*, Plasma Phys. Control. Fusion **51**, 065016 (2009).
- [10] R. Maingi *et al.*, Nucl. Fusion **45**, 1066 (2005).
- [11] T.E. Evans *et al.*, Phys. Rev. Lett. **92**, 235003-1 (2004).
- [12] R.A. Moyer, Phys. Plasmas **12**, 056119 (2005).
- [13] W. Suttrop *et al.*, Phys. Rev. Lett. **106**, 225004 (2011).
- [14] T.E. Evans *et al.*, J. Nucl. Mater. **390-391**, 789 (2009).